ISSN: 2639-7536

Research Article

Petroleum and Chemical Industry International

Bright Spot Validation from 3-D Seismic Data: A Study of Naso-Field, Niger Delta Province, Nigeria

Onyemenam I, Ugwu SA and Nwankwoala HO*

Department of Geology, University of Port Harcourt, Nigeria

***Corresponding author**
Nwankwoala HO, Department of Geology, University of Port Harcourt, Nigeria, E-mail: nwankwoala_ho@yahoo.com

Submitted: 09 Jan 2019; **Accepted**: 29 Jan 2019; **Published**: 05 Feb 2019

Abstract

The validation of identified bright-spots A, B and C on 3D seismic data as Direct Hydrocarbon Indicator (DHI) in Naso field, Niger Delta was achieved through the integration of four surface attributes. These attributes include root mean square, average reflection strength, total energy, and total amplitude which are all amplitude dependent, where region of high value in every attribute indicated possible hydrocarbon prospects. Seismic data and check-shot data were used, which provided positive input for velocity extraction and structural mapping interpretation. A series of NW-SE trending normal growth faults A, B & C were interpreted defining the reservoir structural framework while fault D, E, F & G are post-depositional minor faults which also supported the trapping mechanism. Bright-spot A was mapped between 2,400-2550 milliseconds, while bright-spot B was mapped between 2,600-2,720 milliseconds and bright-spot C between 2,750-3,050 milliseconds. Two hydrocarbon prospects were identified. Prospect-1 was estimated to cover about 907.17, 1323.59 and 1075.44 acres, with subsurface total vertical depth of 9514.3ft, 10499.6ft, 10963ft in BS_A, B & C respectively. Prospect-2 covered about 653.49, 1080.33 and 493.77 acres with subsurface total vertical depth of 8650ft, 9525ft, and 10120ft, respectively. Hence, prospect-1 is considerably more prolific in hydrocarbon yield than prospect-2. The total area of the hydrocarbon prospects in-place has been estimated to about 5,533.79 acres which is likely to yield a prolific reserve for commercial purpose. The gas Chimney and push down highlight the subsurface leakage of gas from a poorly sealed cap rock and show a deep petroleum migration process. The study has been able to validate bright spot during exploration studies in effect to evaluate hydrocarbon reservoir, prospect identification and reservoir prediction.

Keywords: Bright spot, hydrocarbon prospects, structural mapping, growth faults, seismic data, Niger Delta

Introduction

The validation of Bright-Spot from seismic attributes has been initiated and has become an integral part of hydrocarbon exploration study since early 1970s [1]. Tegland stated that "one of the early examples of surface attributes studied and observable as Direct Hydrocarbon Indicator (DHI) is amplitude; it had been preserved in seismic processing" [2].

Bright spot validation is very crucial. This aids in the confirmation of hydrocarbon presence at a particular unit. It is apparently clear that flat spot and bright spot terminate laterally. However, there have been several cases where bright-spot anomalies have been drilled and the target turned out not to be hydrocarbons. Some common "false bright spots" include; volcanic intrusions and volcanic ash layers, highly cemented sands often calcite cement in thin pinch-out zones, low-porosity heterolithic sands and over-pressured sands or shales.

In order to ascertain that identified bright spots are hydrocarbon indicators, the use of several responsive seismic attributes, introduction of texture analysis, 2-D attributes, horizon and interval attributes and the pervasive use of color were introduced as integrals. Bright spot indicator was first used for hydrocarbon exploration around 1970s [3]. This discovery increased interest in varied properties of rock accounting for the pore fluids and how amplitude varied.

The relationship between hydrocarbon and direct hydrocarbon indicator, such as Bright spot has undergone special research concept like amplitude anomalies for delineating hydrocarbon formation by observing sharp amplitude contrast [4].

This study was initiated using data obtained from multinationals operating on major fields in the Niger Delta. The data were imported into the interactive petrel software. The seismic section highlights the fault enclosing the reservoir and indicates the horizon traced on the reflection across the field. Common seismic attributes integrated to achieve the desired results include: Root-Mean-Square (RMS), Total Amplitude, Reflection intensity/Strength and Total Energy. Others are attenuation, velocity pull down and the presence of gas chimneys.

In essence, the aforementioned surface attributes which were used for this study have shown that the field consists of stacked hydrocarbon reservoir prospects characterized by different geological structures. These geological structures which consist of growth faults and rollover anticlines are located around the Niger delta within the northern flank depositional belt and also they are made up of a system of antithetic and synthetic normal faults with compartmentalized reservoir prospect below 8500ft into several blocks of variable size.

The study unravels a robust technique for hydrocarbon identification using amplitude contrast, velocity draw down and gas chimney identification which basically is a result of the interaction of sound waves with hydrocarbon accumulations across the vast area covered by seismic data. The significance of the study is to show the role of seismic surface attributes in the determination of hydrocarbon prospects via validation of bright spots as this is a significant tool in petroleum exploration study. This is as a result of the fact that surface attributes play a key role during location of appraisal and developmental wells in hydrocarbon evaluation and study.

This study will significantly, however, provide detail subsurface structure for delineating new reservoirs that could possibly be discovered in the development of fields. The study will also give insight to detailed understanding of the structure within this location and make further projection on subsequent studies.

Location/Geology of the Study Area

This location designated as NASO field is situated in Escravos River within the fifth depobelt off-shore Niger Delta oil province between latitudes 5o 32' 50" to 5o 40'10" North of the equator and longitudes 5° 8' 10" to 5° 21' 0" East of Greenwich Mean Time (GMT). The Niger Delta is now known as the leading oil province currently in Africa. Up till date, more than 5000 wells have been drilled within the province of Niger Delta [5].Various researches have been done to study the Geology of the Niger Delta basin. Stonely and Burke analysed and accounted for the issue of mega tectonism found within the Niger Delta [6,7]. The Sedimentary tectonic of the tertiary delta was extensively described by Merki; Evamy et al., and Avbovbo [8,9,10].

Burke, stated that "the Current Niger Delta has three well developed submarine networks and several smaller channels which extended to the abyssal plain with other paleo-channels as described by Murat, Omatsola and Cordey [7,11,12]. Clay deposits form a significant seal feature within the complex of Niger Delta province [13, 14]. As stated by Oti and Beka, the deposits of clay in this area have been recognized as provincial seismic marker horizons in the shallow offshore which could be adopted as a correlative tool to correlate stratigraphic event" [15].

Furthermore, Bouvier et al., report on the three dimensional seismic interpretations by employing fault scaling method in the field of the Niger Delta and suggested that the complexities of the subsequent sealing of fault structures were clearly observed and are made plain by day [16].

Various theories and discussion have been put forward for the Niger Delta. For instance, Short & Stauble, Weber and Daukoru concluded that the major factors that control hydrocarbon distribution within the field were literal spill point at the end of discontinuous fault/seal or neither of the two within the planes of fault [17,18].

The evolution of the delta is controlled by Pre and Synsedimentary tectonics the shape of the cretaceous coastline gradually changed as the Niger Delta progresses. This altering coast-line interacted with the Palaeo-circulation configuration and controlled the extent of incursion of the sea [19]. The structural framework of the Niger Delta complex involves the deformation of the overburden sediment due to Synsedimentary truncation in-situ beneath the overburden which is usually activated by gravity, Evamy et al., [9].

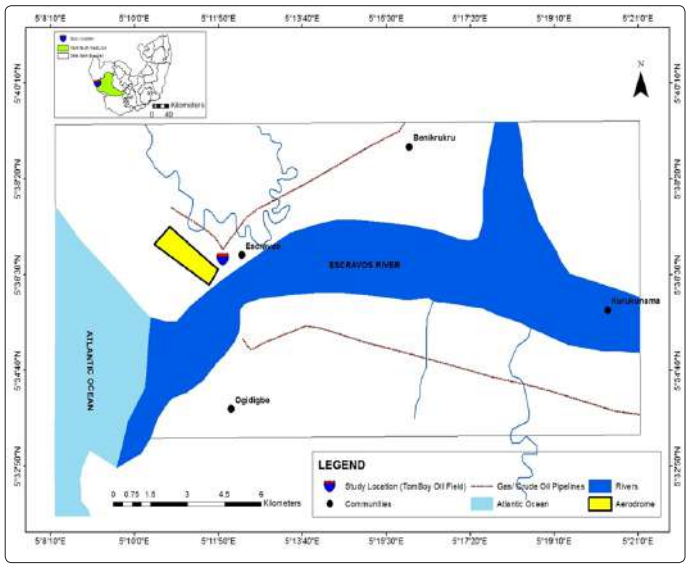

Figure 1a: Area Map of NASO Field, Warri South West Local Government Area, Delta State

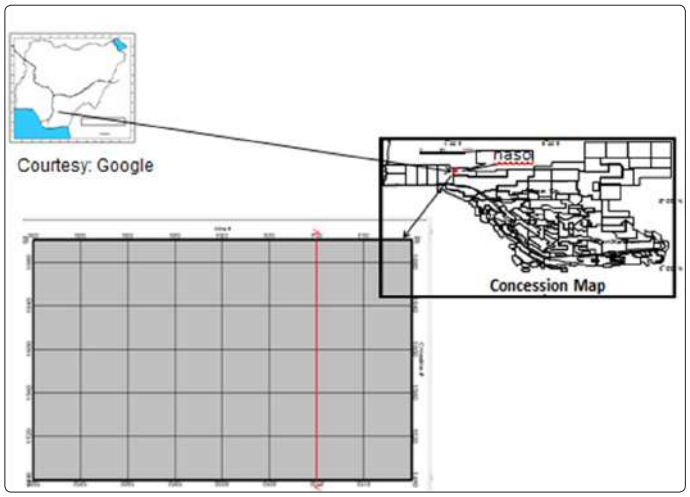

Figure 1b: Base map of the Study Area Showing No Drilled Wells as in the Case of Typical Exploration Study

Oil Migration and Trapping Mechanisms in the Niger Delta

The accumulation of oil and gas are chiefly confined within the Agbada Formation as described by some workers. Doust and Omastsola posited that there are several distributary trends of hydrocarbon in the Niger Delta settings [20]. Most known traps in Niger Delta fields are structural although stratigraphic traps are not uncommon. The structural traps developed during synsedimentary deformation of the Agbada paralic sequence [21].

The primary seal rock in the Niger Delta is the interbedded shale within the Agbada Formation. The shale provides three types of

seals-clay smears along faults, interbedded sealing units against which reservoir sands are juxtaposed due to faulting and vertical seals.According to Waples & Ramly there are two main migration histories proposed for the Niger Delta [22]. For those who favour Agbada Formation the hydrocarbon must have migrated from a short distance up dip to the adjacent sandstone while for the other which favour Akata Formation as the source rock, it is expected that the hydrocarbon migration will be vertical from Akata Formation in to Agbada Formation (reservoir rock). In addition there are two types of migration i.e. vertical and lateral. Fault migration through conductive fault zones have been recognized probably as the most effective way by which hydrocarbon and oil field waters may have migrated into the rollover anticlines. Other mechanisms such as flank of a rollover may have contributed to hydrocarbon accumulation.

It is observed that the dominant trapping mechanism for hydrocarbon pool in the Niger Delta is the crescent shaped growth fault and associated rollover anticlines, the best reservoirs are located in the up thrown side of the growth fault where shale smearing assists in the formation of effective seals by juxtaposition of reservoir against shale [22-24]. Oil and gas reservoirs in NASO Field of the Niger Delta province have come into being over a long period of time as the result of geological processes. The gas and oil have been formed from organic matter and have attained thermal maturity which then migrate into the reservoir rock and trapped by overlying rock formation with very low permeability. This area contains several reservoir units at the subsurface and is prolific and good for hydrocarbon exploration.

Methods of Study

Interpretation Steps:

(i) Project conception
(ii) Loading of 3-D –Seismic data
(iii) Identifications of Bright Spot on Seismic Data; Exploration stage
(iv) Fault interpretation
(v) Subsurface Bright-spots mapping
(vi) Identifying and delineating the structural and stratigraphic features of NASO Field
(vii) Identification of gas chimney and velocity push down
(viii) Identifying hydrocarbon prospects in place

The following surface attributes were integrated to validate bright-spots on 3-D seismics as Direct Hydrocarbon Indications (DHI):

Root-Mean Square Amplitude (RMS)

RMS amplitude is calculated from the average of the square root of the analyzed amplitude. The RMS computation is very sensitive to extreme amplitude values. RMS is an attribute that computes and aids the measure of the degree of reflectivity of the hydrocarbon presence. The RMS is an expression of variation in acoustic impedance [4]. High acoustic impedance indicates high RMS value expressed in stacked and varied lithology.

The RMS Equation is stated below:

$$RMS = \sqrt{\frac{\sum_i^n amp_i^2 * w_i}{\sum_i^n w_i}} \quad (1)$$

Where:

amp = stands for amplitude,
n = denotes the number of samples, while
w = is the weight of each of the amplitude value.

From the above equation, the higher the RMS value the lower the acoustic impedance value which indicates possible presence of hydrocarbon.

Spectural Decomposition (SD)

Spectral decomposition is a way of disintegrating the seismic signatures into its spectral components within a time window of inferred horizon of interest. This component disintegration process aids the clear understanding of the minor subtle faults and channel features [25]. Iso frequency and horizon slides gave rise to three distinct colours – red, green and blue (RGB). The RGB is an additive model where the red, green, and blue colors are combined on different quantities or portions to reproduce other colors [26]. This RGB blending is an effective use of colour that has become an embedded visualization method for seismic attributes. The intensity of each primary colour denotes the level of intensity of the characteristic in that channel.

Average Reflection Strength

Average Reflection Strength (also known as Instantaneous Amplitude) is a complex trace statistic. It is the envelop of the seismic trace, and can be thought of as amplitude independent of phase which is sometimes known as energy envelop, this is regarded as the total or the entire energy of the seismic trace, which depends on phase and its outcome is usually more than or equal to zero it is denoted as:

$$e(t) = [r^2(t) + q^2(t)]\ ½ \quad (2)$$

Where e(t) = energy envelope
r(f) = real seismic trace
q(t) = quadrature seismic trace.

As vividly described by Udohet al, Sweetness/average reflection is a seismic attribute used for detecting sands and sandstones, principally in clastic succession [19].
Sweetness is mathematically denoted below:

$$\text{Sweetness} = \text{Reflection Strength}/(\text{Instantaneous Frequency})^{½} \quad (3)$$

In other to account for the reflection strength, Udoh et al., elucidated that "Reflection strength is amplitude independent of phase, it is continuously positive and has the equivalent range of values as amplitude upon which is obtained [19]. Instantaneous frequency is the measure of the degree of change of phase, has unit of hertz and its connected with the bandwidth of the seismic data and bed thickness [27]. Seismic volume with high amplitude and low frequency denotes high level of sweetness while high frequency and low amplitude signify low sweetness indication. Study by Taner et al., indicates that "Shale unit is typically observed to have low amplitude indicating low acoustic impedance [28]. Shale shows close space reflections meaning high level of frequency [29]. It is characteristically observed that the degree of sweetness is usually very obvious when there is high acoustic impedance difference between sands and shales. Reflection is usually small when acoustic impedance is equally low.

Effective reflection strength

$$Re = \frac{Z_{ss} - Z_{sh}}{Z_{sh}} . h \quad (4)$$

Where Z_{ss} = is the sandstone impedance
h = is the layer thickness
Z_{sh} = is the average shale impedance

$$\frac{N}{G} = \frac{\int_{Z_{zi}}^{Z_{zn}} V_{sand}\, dz}{\Delta Z} \qquad N = \frac{net}{gross} \tag{5}$$

Where $V_{s\,and}$ is the OIL Sand Fraction

Given by

$$V_{sand} = \frac{SI - bAL - a_0}{a_1 - a_0} \tag{6}$$

Where b is the average slope of the shale slope b_o and OIL-sand slope (b_1)
a_0 and a_1 = respective interest in the AI – SI cross-plot
AI = acoustic impedance
SI = shear impedance cross-plot

Total Energy

Total Energy was calculated by summing the squared values of the amplitudes in the analyzed data. The total energy reflection can be related to major lithological changes as well as oil and gas accumulation. This can be employed to differentiate massive reflections from thin-bed composites.

Research indicates that response is not dependent on phase. The response energy is the measure of the amplitude of the reflection strength at the point where the energy envelope is a maximum.

$$RE(t) = \frac{dE(t)^{"}}{dt} - 1^{st}\ \text{derivative} \tag{7}$$

$$RE(t) = \frac{d^2(F(t)}{dt^2} - 2^{nd}\ \text{derivative} \tag{8}$$

Total Amplitude

Total amplitude (integration of amplitude) was calculated by computing the summation of all amplitudes within the analyzed data. The inclusion of total amplitude data in reflection seismic attribute helps to resolve the ambiguity caused in the travel time inversion by the trade-off between reflector position and velocity anomaly. Synthetic models are used to demonstrate the efficacy of amplitude inversion for velocity variation; using the subspace inversion method [27].

The wave front sweep velocity is a measure of the rate at which the incident wave front covers the reflecting boundary Fred [30]. Wave front sweep velocity is very viable for geologic modeling. Conversely, from the wave front sweep velocity method a graphical method evolved, allowing for the utility of compass and ruler to approximation the impact of curvature and diffraction on seismic amplitude. From Zeoppritz equation given by [31]:

$$A = \frac{2Vs^2}{Vp^2}\left[\frac{\Delta\rho}{e} + \frac{2\Delta Vs}{Vs}\right] \tag{9}$$

$$R(\theta) = R(0) - A\,Sin^2\theta \tag{10}$$

$$Asin^2\theta = R(0) - R(\theta) \tag{11}$$

$$A = \frac{R(0) - R(\theta)}{Sin^2\theta} \tag{12}$$

$$R(\theta) = R(0) + Gsin^2\theta \tag{13}$$

Where
R(θ) = Angle of incident
Vp = p-wave velocity obtained within the medium
ΔVp = p-wave velocity difference across interface
Vs = S-wave velocity in medium
ΔVs = S-wave velocity difference across interface
ρ = density in medium
Δρ = density difference across interface
G = referred to the AVO gradient

All the above surface attributes used as Direct Hydrocarbon Indicator (DHI) are amplitude dependent. Presence of hydrocarbon in a formation lowers its velocity and density, thus changing the contrast in acoustic impedance (I) with overlying and underlying formations, hence the reflectivity. In essence, the lowering of the acoustic impedance (I) of a reservoir often produces a high amplitude reflection called *BRIGHT SPOT*, which is the common Hydrocarbon Indicator (HI).

Seismic Chimney and Velocity Push Down

Seismic anomalies such as velocity push down, gas chimneys and Bright Spot are extracted from 3-D seismic data. They are important tools for validation of hydrocarbon exploration and field development. These seismic anomalies are highlighted using a technique that analyzes data with the combination of seismic attribute events. Gas Chimney highlights the migration of gas from deep structure into shallower reservoir and has been used successfully to predict hydrocarbon phase in reservoir rock. Seismic Chimney and push down are usually visible on seismic section and are identified as seismic anomalies, and are characterized by loss of seismic signal as well as areas of low data quality or draw down. The signals are lost due to the break-up of layers or strata resulting to gas escape processes. Seismic Chimneys occur as a result of subsurface leakage of gas from a poorly sealed cap rock. The escape gas causes the overlying rock to have a low density and velocity anomaly which on seismic section are visible directly over a bright spot in a gas bearing layer. Also Chimneys can cut through the bright spot if there is a fault and can continue in the vertical profile. Seismic Chimneys are over the time used as DHI and are associated with push down (velocity anomaly). On seismic section push down are featured with a low seismic velocity such as shale diapir or gas Chimney surrounded by rock with relatively high seismic event [32,33].

After converting these seismic events from time to depth function hydrocarbon indicator will display velocity draw down since the velocity of hydrocarbon is slower than that of rock. Such areas on seismic section are represented or caused by low amplitude [34].

3-D Seismic Data

Using the in-lines and cross-lines, the horizon of interest was mapped across the field within an inline and the cross lines that intersected can be seen (Figure 2). The same holds for all cross lines. Seismic grids were developed as the continuous reflections were picked along the in-lines and cross-lines using the T-Z function.

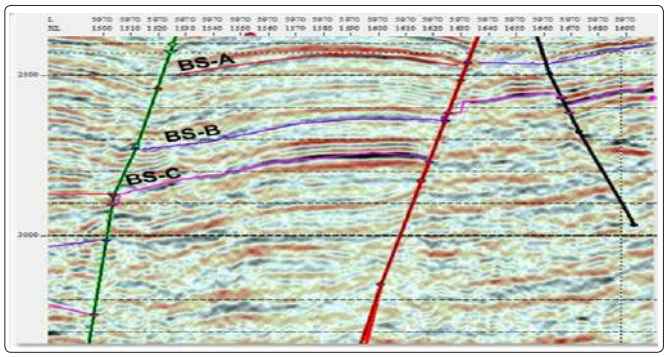

Figure 2: In-line 5970 Cross Section Showing Mapped Growth Faults A, B, C and Identified Picked Bright-Spots (BS-A, B and C)

3-D Seismic Data Acquisition

The purpose of seismic survey is accurately to account for the ground motion caused by an identifiable source in a specific location. The account of ground motion with time constitutes a seismograph and is the basic information used for interpretation through either modeling or imaging. The major procedures are as follows: Generate a seismic pulse with appropriate source, record and display the seismic waveforms on a suitable seismograph and identify the seismic waves in the ground with appropriate transducer. From the above procedure a 3-D seismic data is generated.

3-D Seismic Data Processing

Deconvolution acts along the time axis. It removes the basin seismic wavelengths from various effects of earth and recording system where trace increases temporal resolution by pressing the wavelet. This is followed by stacking the volume of data is reduced to a plane of mid-point-time at zero offset by applying normal move out (NVO) correction to trace from each common depth point (CDP).

More so, migration is utilized to stacked data, a process of moving data elements from midpoint location to subsurface location. It is also called imaging. This improves spatial resolution i.e. bringing the seismic wave into sharper focus. Other secondary techniques are used to improve the effectiveness of the primary process for example dip filter is applied to remove coherent noise in order to stabilize the Auto-correlation. All these steps mentioned above are conventional processing based on certain assumptions. For example when the resolution of the data has been brought to a sharper focus any unwanted or undesirable data can be removed thereby improving the quality of the data before processing. This is also known as data editing.

The field data were recorded in a multiplexed mode using the SEG-Y format. The data were de-multiplexed by transposing a big matrix seismic trace recorded at different offsets with a common shot-point. The transposing stage is the point in which data are converted to a convenient format used throughout the processing. Also involved is the trace editing where noise is trace with transient glitches or mono-frequency signals are deleted.

Data Quality Checking and Importation

Data Quality Checking

In checking for the quality of the data, the major items which include the depth unit coordinates (from both X and Y), the location at which the seismic survey was carried out, company name, type of company and address were taken into consideration.

Data Importation

The data used in this study were imported into the petrel software, where the header was imported first and was matched with appropriate file type. The interpretation of the seismic horizons was done with the in-lines and cross lines of the section. 3-D grid lines were being formed as the seismic horizons were picked. These grids show the displacement of the faults across the section and their trends.

After picking of the seismic horizons, time surface map was produced which was later converted to depth surface map (i.e. T-Z conversion). The major faults were clearly seen from the discontinuities of the reflectors on the seismic section which could be as a result of tectonic or subsurface activities in the area over geologic time.

The synthetic seismogram is an artificial seismic section generated by the assumption that some waveform travels through an assumed model through a given sequence of rock units. It may be considered as the convolution of the assumed source function with a reflectivity function [35]. As stated by Sheriff, "By means of the synthetic seismogram, valuable insights can be obtained into the subsurface geology responsible for a particular seismic event [36]. It represents the acoustic impedance in a layered model. The synthetic seismograms provide a means for tying the well log data with actual seismic record and thus giving a geologic meaning to the seismic data [36]. This would help in studying how seismic character varies as the stratigraphy changes across the basin. "It would also aid in identifying reflections and in determining seismic events that are related to particular boundary surfaces or sequences, generating the synthetic seismogram, involves computing the reflectivity series as function of time from layered acoustic impedances" [35].

The acoustic impedance is derived as a function of one-way time by multiplying digitized sonic velocity and density values at various depth intervals. For a compression wave at normal incidence on the boundary between two media, the reflection coefficient, R is given by the relation below.

$$R = \frac{\rho_2 V_2 - \rho_1 V_1}{\rho_2 V_2 + \rho_1 V_1} \quad (14)$$

$\rho_1 V_1$ and $\rho_2 V_2$ are acoustic impedances of the first and second layers, respectively [37].

According to Ukaigwe (2000), for small acoustic impedance contrasts, the reflection coefficient can be approximated by the relation:

$$R = \frac{\Delta(\rho V)}{2\rho V} \quad (15)$$

From which follows that:

$$R = \frac{\Delta \ln(\rho V)}{2} \quad (16)$$

Seismic Trace = Reflectivity series convolved with a wavelet

$$S(t) = R(t) * b(t) \quad (17)$$

Where R (t) = Reflective Series, b (t) = Convolution or filter and S (t0 = Seismic trace.

Results and Discussions

This research study seeks to prove that bright-spots are often Direct Hydrocarbon Indicators (DHI) on seismic sections. This would be carried out through the integration of different surface attributes which are root mean square (RMS), average reflection amplitude, total reflection amplitude and total energy amplitude. Others are velocity draw down and seismic chimneys.

From the overview perception of the 3-D seismic data administered for this research, three bright spots (A, B, C) were identified. Bright-spot A (BS-A) was mapped between 2,400-2550 milliseconds, while bright-spot B (BS-B) was mapped between 2,600-2,720 milliseconds and bright-spot C (BS-C) between 2,750-3,050 milliseconds. The seismic data has a total number of about 390 In-lines and 220 Cross-lines sections across which the subsurface mapping and interpretation were carried out, as shown in Figure 2.

A total of seven (7) faults were mapped, namely faults A, B, C, D, E, F and G. Only faults A, B and C are visible on a vertical section at inline number 5970 (Figure 2). This is because these faults are concentrated at the western part of the field, and they are the major boundary building faults which define the reservoir closure system encountered in the field as roll-over anticlines. Faults A, B and C are mega growth faults and extend over a considerable distance along the strike, dipping south and visible throughout the seismic section and they intersect the three identified bright-spot horizons A, B and C. Faults D and E are antithetic faults dipping in an opposite sense to the growth faults (A, B, and C) and all died out before inline 6000. A collapsed structure characteristic of the distal portion of the Niger Delta area resulted from antithetic faults D & E dipping in an opposite direction to the faults A and C, hence they form a graben at the middle blocks.

From the surface attribute of mapped bright-spot-A, a region of high RMS amplitude value against an antithetic structural fault (F_D) has been identified as a Direct Hydrocarbon Indicator as shown in Figure 3. The region of high reflection strength/intensity in Figure 4 below typifies area of low acoustic impedance (I) which is an indication of hydrocarbon. Such high reflection has been identified within an area closure against a Growth-Major structural fault (F_A).

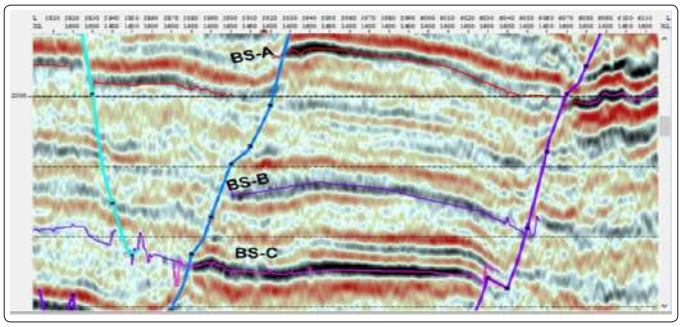

Figure 3: Cross-line 1600 Cross Section Showing Mapped Growth Faults and Identified Picked Bright-Spots A, B and C

Also in Figure 5, region of high energy is a Direct Hydrocarbon Indication because energy is directly proportional to amplitude in fluids bearing formation, which has been identified on the surface attribute closing against an antithetic structural fault (F_D).Amplitude is inversely proportional to the change in acoustic impedance, hence a zone bearing hydrocarbon usually has high amplitude and low impedance. From the mapped bright-spot as in the case of figure 6 below, a zone of high amplitude value closing against an antithetic fault (F_D) has been identified as Direct Hydrocarbon Indicator.

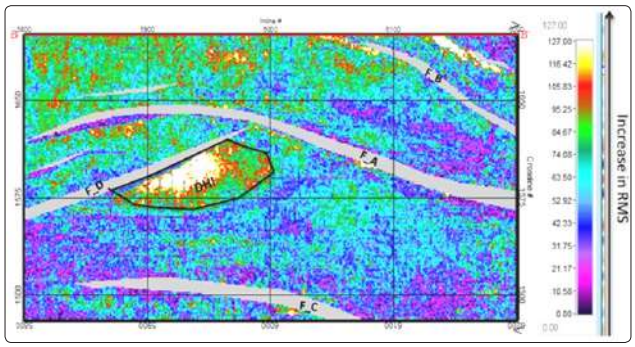

Figure 4: Validation of Bright Spot-A as Direct Hydrocarbon Indicator on Root Mean Square (RMS), 3-D Seismic Attribute

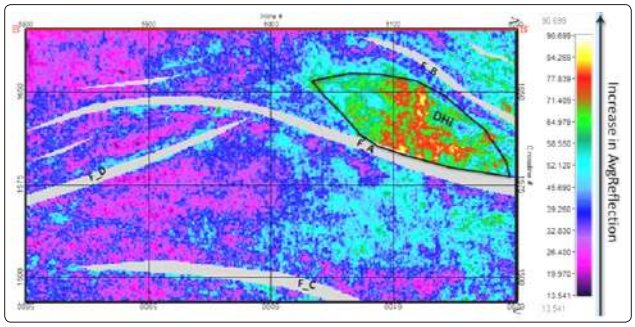

Figure 5: Validation of Bright Spot-A as Direct Hydrocarbon Indicator on Average Reflection Coefficient, 3-D Seismic Attribute

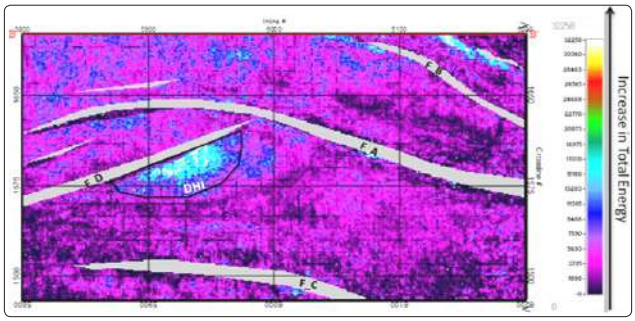

Figure 6: Validation of Bright Spot-A as Direct Hydrocarbon Indicator on Total Energy 3-D Seismic Attribute

The super-impositions of both reflection strength and amplitude attributes on depth top structural map, (Figure 7 and 8 respectively) showed zones of bright-spots within a fault dependent structural closure. This validates the bright spot (BS_A) as a Direct Hydrocarbon Indicator. The top depth structural and isopach maps Figures 9 &10 have obviously defined the structural closures of the two hydrocarbon prospects at this horizon level designated as BS_A. Prospect-1 & 2. From the isopach map (Figure 10) the prospects 1 and 2, the estimated areas in subsurface are 907.17 and 653.49 acres, respectively.

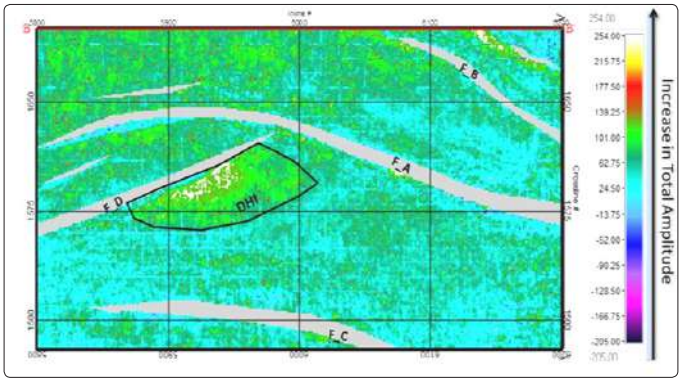

Figure 7: Validation of Bright Spot-A as Direct Hydrocarbon Indicator on Total Amplitude, 3-D Seismic Attribute

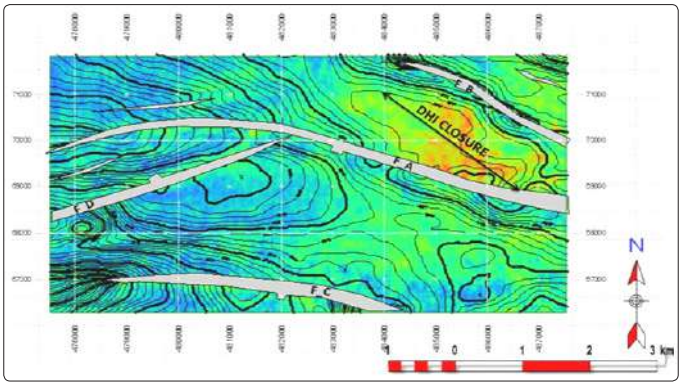

Figure 8: Super-Imposition of Reflection Strength Attribute on Top Depth Structure Map

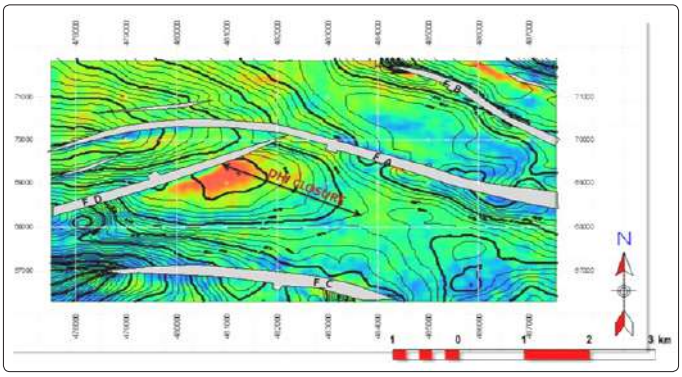

Figure 9: Super-Imposition of Total Amplitude on Top Depth Structure Map

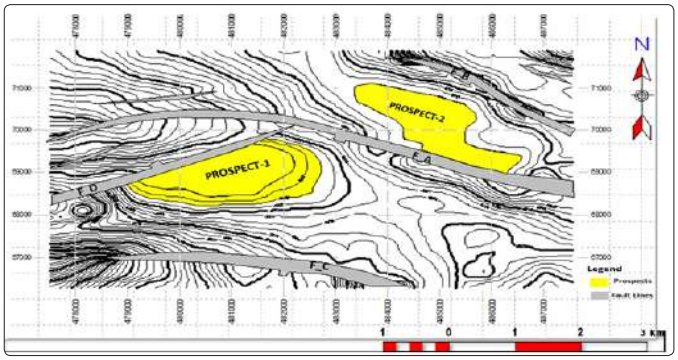

Figure 10: BS_A Top Depth Structural Map Showing Mapped Hydrocarbon Prospects

Bright-spot B (BS_B) also through the integrations of the four aforementioned seismic attributes two prospective hydrocarbon zones 1 and 2 were identified. From RMS amplitude, two zones were directly identified to have high RMS values. They are interpreted to be Direct Hydrocarbon Indicators. These two regions constituted Roll-over Anticlinal Fault Dependent Closures, (Figure 11). Also, region of high reflection strength typifies area of low acoustic impedance (I) which is an indication of the presence of hydrocarbon (Figure 12). According to Rotimi et al., amplitude, average reflection strength and spectral decomposition are useful tools for locating reservoir quality, outlining their geometry and possibly displaying lateral changes in thickness [38].

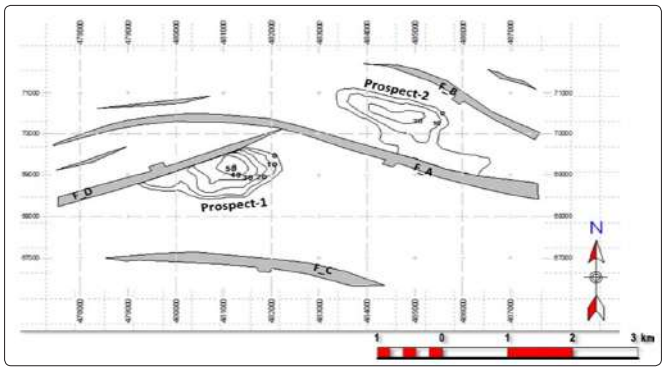

Figure 11: Isopach Map of Prospects 1 and 2 Identified on Mapped Bright-Spot A

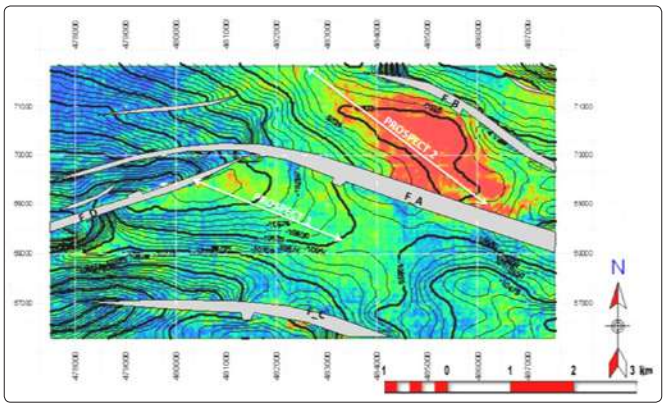

Figure 12: BS_B Top Depth Structural Map Showing Mapped Hydrocarbon Prospects, 1 and 2

The super-imposition of the total amplitude attribute on the top depth structural map actually defines the geometry of the prospects 1 & 2 closures. Prospect 1 closed on Fault A and D (antithetic to F_A) while prospect 2 closed on Fault B (synthetic to F_F), hence, a two-way roll-over fault dependent system was formed Figure 13, 14 and 15. From the interpretation, considerable areas of prolific hydrocarbon accumulation have been estimated for prospect-1 and 2 as 3,306.20 acres and 2,227.59 acres respectively. Therefore a total estimated area of 5533.79 acres which is likely to yield a prolific reserve for commercial purpose has been an important part of the study.

From the seismic data, the identified gas chimneys and velocity push down have provide additional prospect evaluation and validation as direct hydrocarbon indicator. From in-line 5970 cross section (Figure

13) the horizon discontinuity is associated with fault line, the chimney must have been caused by gas leakage from the subsurface which cut across 2 identify Bright-spot (B & C) as show in the seismic profile due to a leaking fault system (Figure 14). According to Barthold et al., any alternative explanation for the loss of seismic signal would be the actual break-up of layering resulting from fluid escape processes [39]. In addition one of the identified chimneys terminates at BS(C) which indicates the migration of gas from a deeper section in the field. It is most likely that the gas trapped in the reservoir migrated up dip (westward) from the deeper part of the growth fault system. Anywhere there are Bright-Spots and associated hydrocarbon prospect there is a push down as such as direct hydrocarbon indicator which is caused by the presence of hydrocarbon fluid in the reservoir rock surrounded by rock with relatively high seismic event, which have provided valuable insight for hydrocarbon identification and understanding of deep petroleum migration processes.

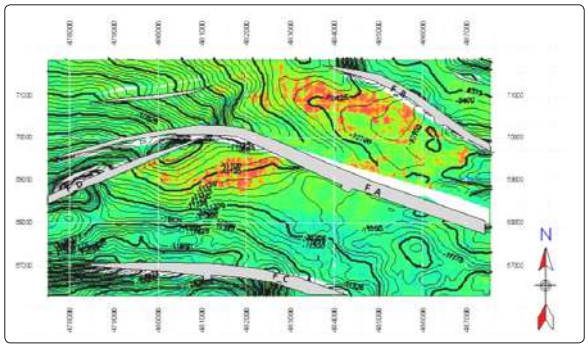

Figure 13: Super-Imposition of Total Amplitude on Top Depth Structure Map

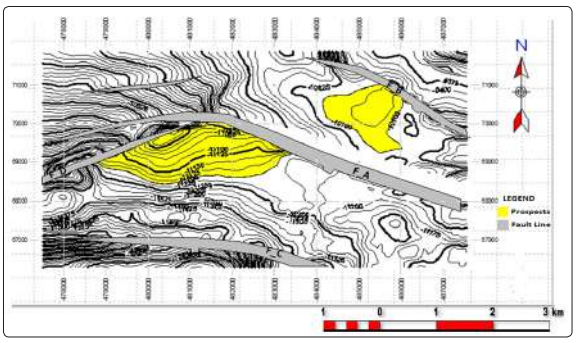

Figure 14: BS_C Top Depth Structural Map Showing Mapped Hydrocarbon Prospects

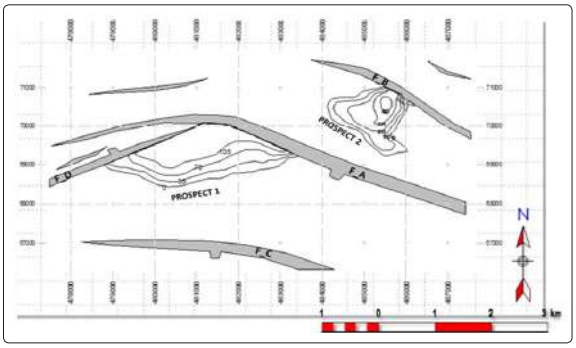

Figure 15: Isopach Map of Prospects 1 & 2 Identified on Interpreted Bright-Spot C

Table 1: Summation of Hydrocarbon Prospects

BRIGHT SPOTS	PROSPECT 1	PROSPECT 2
BS_A	907.17 acres	653.49 acres
BS_B	1,323.59 acres	1,080.33 acres
BS_C	1,075.44 acres	493.77 acres
TOTAL	3,306.20 acres	2,227.59 acres
GRAND TOTAL	**5,533.79 acres**	

Table 2: Summation of Prospect Depth in TVDSS

BRIGHT SPOTS	PROSPECT 1 (FT)	PROSPECT 2 (FT)
BS (A)	9514.3	8650
BS (B)	10499.6	9525
BS (C)	10963	10120
TOTAL	30976.9	28295

Table 3: Summation of Prospect Evaluation

BRIGHT SPOT	DATA INTERPRETED	NUMBER OF SECTION	MAPPED BRIGHT SPOT (MS)	HYDROCARBON PROSPECT		TV DSS (FT)	
				P(1) acres	P 2 acres	P 1 ft	P 2 ft
BS_A	55.6KM^2	390 in line 220 x –line sections	2,400 - 2550	907.17 acres	653.49	9514.3	8665
BS_B			2600 - 2720	1323.59	1080.33	10499.6	9525
BS_C			2750 - 3050	1075.44	493.77	10963	10120
TOTAL				3306.20	2,227.59	30976.9	28295
GRAND TOTAL				5,533.79 acres			

Summary and Conclusion

The research involved evaluation and identification of Bright Spots as hydrocarbon prospects and its provision of a comprehensive knowledge of the subsurface geologic structure in Naso Field. Four seismic attributes were used to identify bright spot horizons. These are the Root Mean Square (RMS), Total amplitude, Total energy, Average reflection strength/intensity. Others are Velocity Push Down and Seismic Chimneys. All the Bright Spots identified were seen on attribute surface horizon as high amplitude zones. The 3-D seismic data used for this research comprised of a total number of about 390 inline and 220 cross line sections. They were used to map the lateral continuity of the hydrocarbon prospects observed in the Field. Three bright spot horizons were identified as BS (A, B and C) BS_A was mapped between 2400-2550 milliseconds, BS_B was mapped between 2600-2720 milliseconds, BS_C was mapped between 2780-3050 milliseconds. From the 3-D subsurface structural interpretation seven faults were delineated but only faults A, B and C were visible and these cut through the vertical section of inline number 5970. The entrapment of hydrocarbon in the field was controlled by the growth fault and roll-over anticlinal closures which trend mainly in NW-SW direction. Others trend in the NE-SW direction [40-42].

In Naso Field 2 hydrocarbon prospects were identified with area of prolific hydrocarbon accumulations estimated for prospect (1) as 3306.20 acres and for prospect 2 as 2227.59 acres respectively, amounting to a total estimate of 5533.79 acres. This extensive area can most likely yield a prolific reserve for commercial purpose. More so, the subsurface total vertical depth for prospect 1 was estimated as (30976.9ft) and for prospect 2 as (28295ft) respectively. The difference between the depth values show that prospect 2 falls on the up thrown part of the growth fault defining the reservoir, hence values on the up thrown portion is relatively shallower than the downthrown blocks. The western part of the field is a highly prospective area with high amplitude gas observed to migrate upwards due to a leakage of the fault system which leads to gas Chimneys and velocity push down observed as Direct Hydrocarbon Indicators.

The study has been able to depict the importance of identification and validation of bright-spots during exploration seismological studies, aimed at the evaluation of hydrocarbon exploration and reservoir characterizations. The presence of the two-way faulted anticlinal closure constitutes the main hydrocarbon structural framework which defines the reservoir trapping system in the area. The synergistic interpretation and integration of seismic attributes have made the study both very qualitative and quantitative, as information missed by any of the attributes is complemented for by the other, thereby necessitating a justifiable conclusion.

It can be said that the mega growth faults (A, B and C) which occurred across an anticlinal structure can be significant in the creation of multiple reservoir traps, which are therefore the ultimate target in well positioning. From the seismic profile it is clear that gas chimney and velocity push down were extracted and used to understand the migration pathway and distribution of hydrocarbon in the field. The seismic chimney cut across the three bright spot horizons. From the respective top depth structure map the bright spots identified fall within a two way fault dependent roll-over structural closure, validating the bright-spots as Direct Hydrocarbon Indicators (DHI).

Furthermore, the surface attributes and depth top structural maps of the mapped bright spots-A, B and C have indicated the presence of direct hydrocarbon prospects in the study field. It can therefore be concluded that the total area of the hydrocarbon prospects in-place has been estimated to about 5,533.79 acres. This is likely to yield a prolific reserve for commercial purpose. Naso field is made up of a system of antithetic and synthetic normal faults with compartmentalized reservoir prospects below 8500ft into several blocks of variable sizes. Based on the results of the study, the following are recommended:

1. For definite reserve estimation of the field, comprehensive reservoir evaluation and study should be carried out to know its viability at commercial quantity.
2. Seismic attributes are used generally for reservoir prediction in hydrocarbon prospect, optimization of field development, exploration and for proper decision making.
3. A good point of interest should be where the amplitude reflection is high, the higher the bright-spot, the better the prospect and the higher the hydrocarbon saturation. Exploration/Appraisal wells should be drilled in areas of identified prospects.

References

1. Chopra S, Marfurt K (2005) Seismic attribute. A historical perspective, Geophysics, 70: 3SO-28SO.
2. Tegland ER (1973) Utilization of computer-derived seismic parameters in direct hydrocarbon exploration and development, in Lithology and direct detection of hidrocarbon using geophysical methodos: Dallas Geophysical an Geological Societies symposium.
3. Hammond AL (1974) Bright spot: better seismological indicators of gas and oil Science 185: 515-517.
4. Brown AR (2010) Dim Spots in Seismic Images as Hydrocarbon Indicators Search and Discovery Article 1-3.
5. Raji AY, Abejide TS (2013) Shell D'arcy Exploration & The Discovery Of Oil As Important Foreign Exchange Earnings In Ijawland Of Niger Delta, C. 1940s-1970 Arabian Journal of Business and Management Review (OMAN Chapter) 2: 11.
6. Stoneley R (1966) Introduction to Petroleum exploration for non-geologists: Oxford University Press 119.
7. Burke K (1972) Long shore drift, submarine canyons and submarine fans in Development of Niger Delta. American Association of Petroleum Geologists Bulletin 56: 1975-1983.
8. Merki PJ (1970) Structural Geology of the Cenozoic Niger Delta. African Geology, University of Ibadan Press 251-268.
9. Evamy BD, Haremboure J, Kamerling P, Molloy FA, Rowland PH (1978) Hydrocarbon habitat of tertiary Niger Delta: AAPG Bulletin 62: 1-39.
10. Avbovbo AA (1978) Tertiary Lithostratigraphy of Niger Delta. AAPG Bulletin. 62: 295-306.
11. Murat RC (1970) Stratigraphy and Paleogeography of the Cretaceous and Lower Tertiary in Southern Nigeria. African Geology, University of Ibadan Press 635-648.
12. Omatsola ME, Cordey WC (1976) The Afam Formation, its Stratigraphy, Microfauna and Environment of Deposition. SPDC unpublished Report.
13. Nwangwu U (1990) A unique, hydrocarbon trapping mechanism in the offshore Niger Delta, in Oti, M.N., and G. Postma, eds., Geology of Deltas: Rotterdam, A. A. Balkema, 269-278.
14. Reijers TJA, Peters SW Nwajide CS (1997) The Niger Delta Basin. African Basins, in Sedimentary basins of the world 3: 151-172.

15. Beka FT, Oti MN (1995) The distal offshore Niger Delta: frontier prospects of a mature petroleum province, in Oti, M.N. and Postima. G.Ed, Geology of Deltas: Rotterdam. A.A. Bulkema 237-24.
16. Bouvier JD, Sijpeisteijn K, Kluesner DF, Onyejekwe CC, Van der Pal RC (1989) Three-dimensional Seismic Interpretation and fault: Sealing Investigations, Nun River Field Nigeria: The American Association of Petroleum Geologist Bulletin 73: 1397-1414.
17. Short KC, Stauble AJ (1967) Outline Geology of Niger Delta: AAPG Bulletin 51: 761-779.
18. Weber KJ, Daukoru EM (1975) Petroleum geology of the Niger Delta: 9th world Petroleum Congress Proceedings 2: 209-221.
19. Udoh MU, Udofia P, Akpan MO, Das UC (2017) High Resolution Sequence Stratigraphy, Sedimentology and Paleoenvironmental Studies of Late Eocene – Late Oligocene Sediments, Greater Ughelli Depobelt, Niger Delta, Nigeria. International Basic and Applied Research Journal 3: 1-32.
20. Doust H, Omatsola E (1990) Niger Delta in Edwards JD and Santogrossi, P.A., eds. Divergent/passive margin Basins, AAPG Memoir 48; Tulso, America Association of Petroleum Geologists 239-248.
21. Adedapo JO, Ikpokonte AE, Schoeneich K, Kurowska E (2014) An Estimate of Oil Window in Nigeria Niger Delta Basin from Recent Studies American International Journal of Contemporary Research 4: 114-121.
22. Waples DW, Ramly M (2001) A statistical method for correcting log-derived temperatures. Petroleum Geoscience 7: 231-240.
23. Kurowska E, Schoeneich K (2010) Geothermal Exploration in Nigeria. Proceedings of World Geothermal Congress. Bali, Indonesia 25-29.
24. Ochuko A (2011) Determination of Geothermal Gradient and Heat Flow Distribution in Delta State, Nigeria. Intern Journal of the Physical Science. 6: 7106-7111.
25. Brown AB (2001) Understanding seismic attributes. Geophysics 66: 47-48.
26. Frery AC, Perciano T (2013) Introduction to image processing using R-learning by examples.
27. Yanghua W, Gregory AH (1995) Tomographic inversion of reflection seismic amplitude data for velocity variation. Geophysical Journal International 123: 355-372.
28. Taner MT, Schuelke JS, Doherty OR, Boysal E (1994) Seismic attribute revisited.64th Annual Inlt. Meeting. SEG Expanded Abstracts 94: 1104-1106.
29. Taner MT, Sheriff RE (1977) Application of amplitude, frequency and other attributes to stratigraphic and hydrocarbon determination: in C.E. Peyton, (ed), AAPG Memoir 26, Seismic stratigraphy – applications to hydrocarbon exploration 301-327.
30. Fred JH (1975) Amplitude of Seismic Waves- A Quick Look. Geophysics 40: 745-762.
31. Zoeppritz K (1919) Erdbebenwellen VIII B, Über Reflexion ad Durchgang seismischer wellen durch Unstetigkeitsflachen: Göttinger Nach 66-84.
32. Heggland R, Meldahl P, de Groot P, Aminzadeh F (2000) Chimneys in the Gulf of Mexico. The American Oil and Gas Reporter 78-83.
33. Meldahl P, Heggland R, Bril AH, de Groot PFM (2001) Identifying targets like faults and chimneys using multi-attributes and neural networks, The Leading Edge.
34. Fred A, David C (2003) Seismic Meta-Attributes as a Practical Exploration Tool: Gas Chimney and Fault Volumes Search and Discovery Article #40101 AAPG Explorer.
35. Kearey P, Brooks M (2000) An Introduction to Geophysical Exploration: Blackwell science Ltd 254.
36. Sheriff RE (1977) Limitations on resolution of seismic reflections and geologic detail derivable from them in seismic stratigraphy-Applications to Hydrocarbon Exploration (ed. By C.E Payton). Memoir of the America Association of Petroleum Geologists, Tulsa, 22.
37. Gadallah M (1994) Reservoir Seismology Geophysics in Nontechnical Language a: Penn Well Publishing Company, Tulsa, Oklahoma 382.
38. Rotimi OJ, Ameloko AA, Adeoye OT (2010) Applications of 3-D Structural Interpretation and Seismic Attribute analysis to Hydrocarbon Prospecting over X-field Niger Delta. International Journal of Basic & Applied Sciences 10: 36-54.
39. Barthold MS, Gerard TK, Ruud TES (2004) Surface and subsurface expression of gas seepage to the seabed examples from the Southern North Sea. Marine and petroleum Geology 22: 499-515.
40. Stacher P (1995) Present understanding of the Niger Delta hydrocarbon habitat. In M. N. Oti & G. Postma (Eds.), Geology of deltas, Rotterdam: A. A. Balkema 257-267.
41. Ukaigwe NF (2000) A first Course in Seismic Exploration: Published in Nigeria by Eddy-Joe Publishers 417.
42. Weber KJ (1971) Sedimentological aspects of oil fields in the Niger Delta. Geologie en Mijnbouw 50: 559-576.